On the high-fidelity monitoring of C_3 and C_4 crops under nutrient and water stress

Gladimir V. G. Baranoski[a], Tenn F. Chen[a], Bradley W. Kimmel[a], Erik Miranda[a] and Daniel Yim[a]

[a]Natural Phenomena Simulation Group, School of Computer Science, University of Waterloo, 200 University Avenue West, Waterloo, Canada

ABSTRACT

The different photosynthetic and morphological characteristics of C_3 and C_4 plants may lead to distinct physiological responses of C_3 and C_4 crops to stress factors. These responses are strongly correlated with the red edge of these plants, the s-shaped curve in the 680-800nm region of their reflectance spectra. We performed controlled *in silico* experiments to investigate the patterns of the red edge displacements resulting from C_3 and C_4 specimens subjected to the same stress conditions. Our findings indicate these patterns need to be taken into account in the development of effective monitoring procedures for C_3 and C_4 crops.

Keywords: Plant leaves, reflectance, red edge position, stress factors, simulation.

1. INTRODUCTION

Earth's fresh water supplies are used predominantly in agriculture. This situation makes the effective monitoring of crop responses to nutrient and water stress essential not only from an economical, but also from an ecological point of view. An underestimation of their nutrient and water requirements may lead to reduced yields, while an overestimation may lead to adverse human health and environmental effects such as the contamination (*e.g.*, due to the excessive use of fertilizers) and even depletion of limited fresh water supplies.[1,2] These aspects have motivated the use of remotely sensed data as a tool to distinguish between nutrient and water stress in precision crop applications,[3–5] and the development of accurate drought stress detecting sensors to limit irrigation water use and prevent long-term production losses.[6] It is worth noting that the high demand for reliable early detection of stress conditions is not limited to agricultural applications. It is also desirable in land rehabilitation applications and forestry.[7] For example, certain fungal diseases responsible for massive tree mortality in forests can cause a stoppage of sap flow, which, in turn, results in wilt. Hence, it is possible to detect these diseases at an early stage by assessing the water stress conditions in the affected vegetation.[8]

Two different photosynthetic mechanisms can be found in high order plants, namely the single cell C_3 photosynthetic pathway and the two cell C_4 photosynthetic pathway.[9] Although C_3 species (*e.g.*, rice and soy) are more numerous than C_4 species (*e.g.*, sorghum and corn), the latter account for approximately a quarter of the world's agricultural production.[10] This can be largely attributed to their higher photosynthetic capacity, which has motivated recent investigations aimed at the introduction of the C_4 photosynthetic pathway into C_3 crops such as soy and rice.[9,10] The different biophysical characteristics of C_3 or C_4 plants may lead to distinct responses to stress factors. These responses are strongly correlated with their red edge, the s-shaped curve in the 680-800nm region of their reflectance spectra.[11] The point of maximum slope of this curve, known as the red edge position (REP), corresponds to the peak of its first derivative, which can be obtained by computing the point of intersection of its second derivative with the abscissa.[12] Nutrient and water stress can result in a REP shift, notably toward shorter wavelengths, known as "blue shift".[8] Accordingly, red edge data can be used, for example, in the online control of nitrogen (N) spreading (N fertilization treatments), and to assess water status.[4,5] It has been observed[13] that a REP shift of only one nanometer may translate to a difference in nitrogen fertilizer requirement of approximately 15 kg/ha. It is also worth noting that although water stress may have a positive effect on the sugar contents of some crops (*e.g.*, fruits, green soy and sweet potatoes), a more severe reduction of water content lay lead to a decline in crop yield and fruit size.[8]

In this work, we performed controlled *in silico* experiments to investigate the patterns of the red edge displacements resulting from C_3 and C_4 plants subjected to the same nutrient and water stress conditions. For this investigation, we have selected two species representative of C_3 and C_4 plants, namely soy (*Soja Hispida*) and corn (*Zea mays L.*). This choice was motivated by two aspects. First, their significant agricultural value, which also translates to a larger availability of measured data for these species in the scientific literature. Second, the fact that their leaves
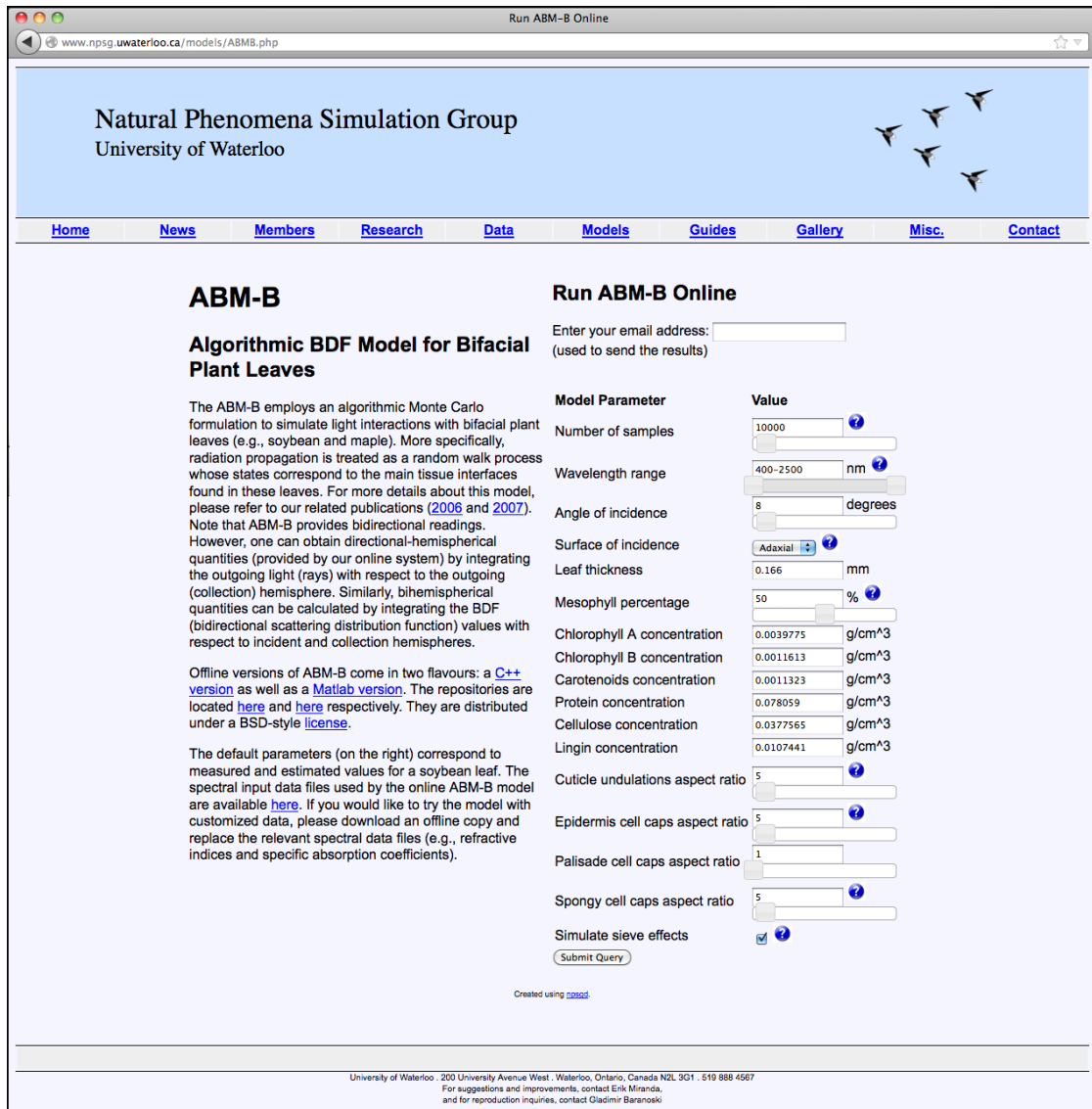
Figure 1: The web interface for the ABM-B model available through the Natural Phenomena Simulation Group Distributed (NPSGD) framework.[14] Through the webpage, researchers can configure biophysical parameters and execute light transport simulations involving bifacial C_3. The default values depicted for these parameters were used in our *in silico* experiments involving a typical soy leaf.

have a distinct morphology, bifacial and unifacial, respectively, which enables a broader examination of biophysical phenomena leading to REP shifts. Our findings indicate that specific REP shift patterns need to be taken into account in the development of effective monitoring procedures for C_3 and C_4 crops in order to accurately assess their irrigation and nutrient requirements.

2. MATERIALS AND METHODS

Our *in silico* experiments were performed using predictive spectral models of light interaction with bifacial and unifacial plant leaves, namely the ABM-B (algorithmic BDF (bidirectional scattering distribution function) model for bifacial plant leaves) and the ABM-U (algorithmic BDF model for unifacial plant leaves), respectively. The descriptions of these models are fully provided in the scientific literature.[15, 16] In order to allow the reproduction and extension of our investigation to other experimental conditions, we made the simulation framework and data employed in this work openly available for download.[17–19] Hence, researchers can either download offline versions of the ABM-B and ABM-U models and perform the simulations on their own computers, or run the simulations through our online system[14] (Figs. 1 and 2, respectively).

Natural Phenomena Simulation Group
University of Waterloo

Home News Members Research Data Models Guides Gallery Misc. Contact

ABM-U

Algorithmic BDF Model for Unifacial Plant Leaves

The ABM-U employs an algorithmic Monte Carlo formulation to simulate light interactions with unifacial plant leaves (e.g., corn and sugar cane). More specifically, radiation propagation is treated as a random walk process whose states correspond to the main tissue interfaces found in these leaves. For more details about this model, please refer to our related publications (2006 and 2007). Note that ABM-U provides bidirectional readings. However, one can obtain directional-hemispherical quantities (provided by our online system) by integrating the outgoing light (rays) with respect to the outgoing (collection) hemisphere. Similarly, bihemispherical quantities can be calculated by integrating the BDF (bidirectional scattering distribution function) values with respect to incident and collection hemispheres.

Offline versions of ABM-U come in two flavours: a C++ version as well as a Matlab version. The repositories are located here and here respectively. They are distributed under a BSD-style license.

The default parameters (on the right) correspond to measured and estimated values for a corn (maize) leaf. The spectral input data files used by the online ABM-U model are available here. If you would like to try the model with customized data, please download an offline copy and replace the relevant spectral data files (e.g., refractive indices and specific absorption coefficients).

Run ABM-U Online

Enter your email address: [   ]
(used to send the results)

Model Parameter	Value	
Number of samples	10000	
Wavelength range	400–2500	nm
Angle of incidence	8	degrees
Surface of incidence	Adaxial	
Leaf thickness	0.204	mm
Mesophyll percentage	80	%
Chlorophyll A concentration	0.002895146	g/cm^3
Chlorophyll B concentration	0.00079866	g/cm^3
Carotenoids concentration	0.000658895	g/cm^3
Protein concentration	0.05308714	g/cm^3
Cellulose concentration	0.05318708961	g/cm^3
Lingin concentration	0.00605852938	g/cm^3
Cuticle undulations aspect ratio	10	
Epidermis cell caps aspect ratio	5	
Spongy cell caps aspect ratio	5	
Simulate sieve effects	☑	

Submit Query

Created using npsgd.

University of Waterloo . 200 University Avenue West . Waterloo, Ontario, Canada N2L 3G1 . 519 888 4567
For suggestions and improvements, contact Erik Miranda,
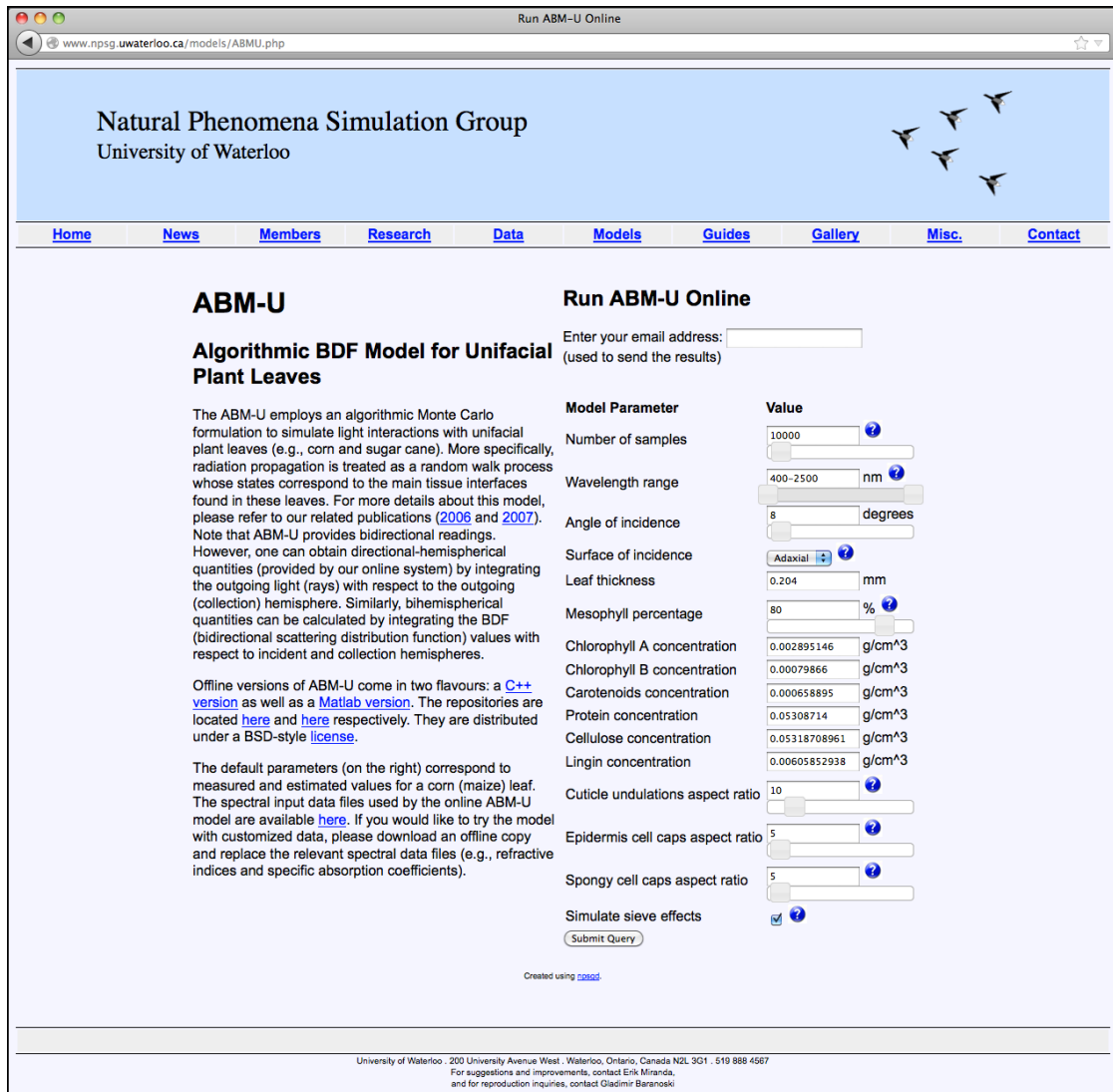and for reproduction inquiries, contact Gladimir Baranoski.

Figure 2: The web interface for the ABM-U model available through the Natural Phenomena Simulation Group Distributed (NPSGD) framework.[14] Through the webpage, researchers can configure biophysical parameters and execute light transport simulations involving C_4 plants with unifacial leaves. The default values depicted for these parameters were used in our *in silico* experiments involving a typical corn leaf.

In order to characterize a typical soy leaf and a typical corn leaf, we used data provided in the scientific literature.[20–22] This data along with simulation parameters (wavelength range and angle of incidence) were configured using the web interfaces presented in Figs. 1 and 2, respectively. The modelled spectral responses employed in our investigation correspond to directional-hemispherical reflectances (ρ) obtained from the adaxial leaf surfaces, and considering an angle of incidence of 8° and a spectral resolution of 5 nm. With respect to the stress conditions, our investigation focused on moderate water stress and nitrogen deficiency.

We considered moderate water stress (relative water content around or above 70%) for two reasons. First, it occurs more often in nature.[23] Second, we are aiming at early detection of stress factors so that irreversible or slowly reversible damages to the plants' photosynthetic apparatus, that are likely to occur during severe water stress,[24, 25] can be prevented. Accordingly, we simulated two levels of moderate water content reduction, namely 15% and 30%. In the case of the soy leaf, this change of water content resulted in its thickness being reduced to 92.5% and 77.5%, respectively. These figures were estimated from experimental work performed by Woolley.[26] Similarly, in the case of the corn, the change in water content resulted in its thickness being reduced to 87.5% and 75%, respectively, and the aspect ratio of its spongy cells being increased by 14% and 33%, respectively. These figures were also estimated from experimental work performed by Woolley.[26, 27]

Similarly, our decision to simulate nutrient stress through nitrogen deficiency was motivated by the following reasons. First, the majority of nutrient stress symptoms have a similar effect on foliar spectral responses.[28, 29] Second, nitrogen is arguably the most important element for growing crops and maintaining a healthy environment.[30] Finally, it is the mineral nutrient required in the greatest amount by plants.[1] We also remark that the effects of mineral nutrients on crop yield and their connection with plant water stress have been examined in the literature mainly through studies involving nitrogen-deficient plants.[3–5, 31] As stated by Carter and Knapp,[32] nitrogen deficiency can be closely simulated by varying the pigment concentration of modelled leaves. Accordingly, we reduced the pigment concentrations of our modelled normal (control) specimens by 15% and 30% to obtain the spectral responses for the modelled nitrogen-deficient specimens.

We employed the following central-difference second order formulas[33] for the first (Equation 1) and second (Equation 2) derivatives of the modelled directional-hemispherical reflectance curves in order to estimate the REP for these curves:

$$\rho'(\lambda) = \frac{\rho(\lambda + h) - \rho(\lambda - h)}{2h} \qquad (1)$$

and

$$\rho''(\lambda) = \frac{\rho(\lambda + h) - 2\rho(\lambda) + \rho(\lambda - h)}{h^2}, \qquad (2)$$

where λ corresponds to the wavelength of interest and h represents the step size. In our numerical computations of the derivatives, we considered a step size of 25 nm.

3. RESULTS AND DISCUSSION

In our first set of simulations, we have considered typical corn and soy specimens submitted to two different levels (15% and 30%) of nitrogen deficiency and water reduction. As expected, the results presented in Figs. 3 to 6 and Table 1 indicate a monotonic shift toward shorter wavelengths. However, a closer examination of the REP values indicates that while nitrogen deficiency resulted in an approximately linear decrease of the REP for both specimens, the water reduction resulted in a different pattern. More specifically, while for the corn specimen the decrease was also approximately linear, for the soy specimen the decrease was approximately quadratic as highlighted by the REP differences (from normal to 15% and from 15% to 30%) presented in Table 2.
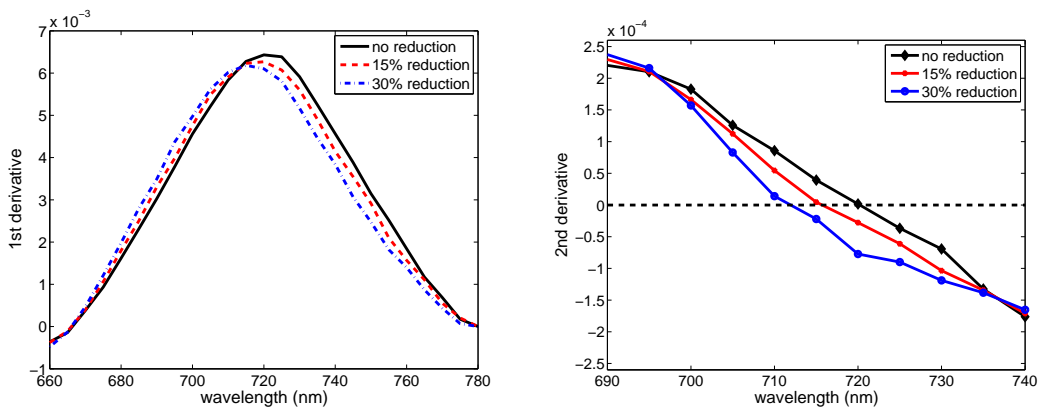

Figure 3: Simulated changes in the REP of a typical corn specimen due to nitrogen deficiency. Left: first derivative of the reflectance spectra. Right: second derivative of the reflectance spectra.
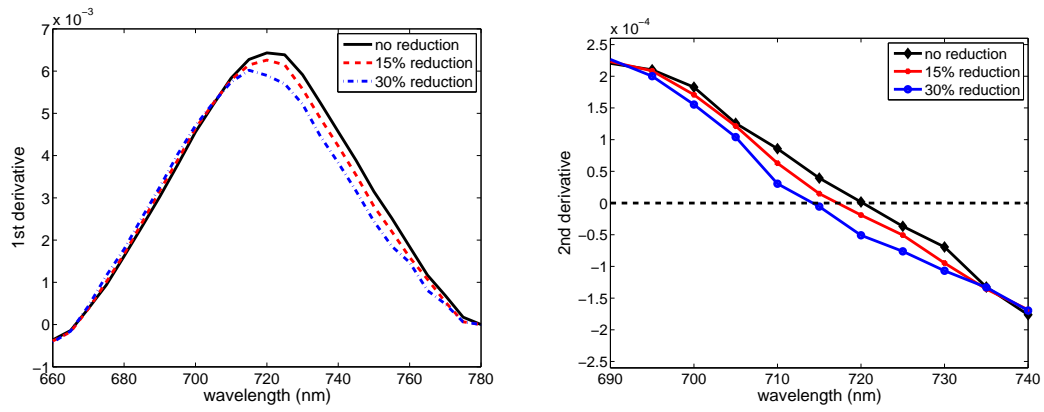
Figure 4: Simulated changes in the REP of a typical corn specimen due to moderate water reduction. Left: first derivative of the reflectance spectra. Right: second derivative of the reflectance spectra.
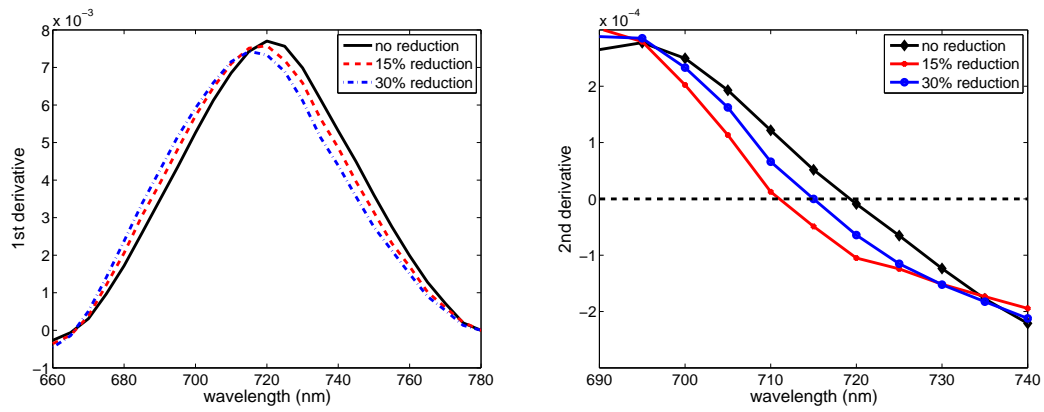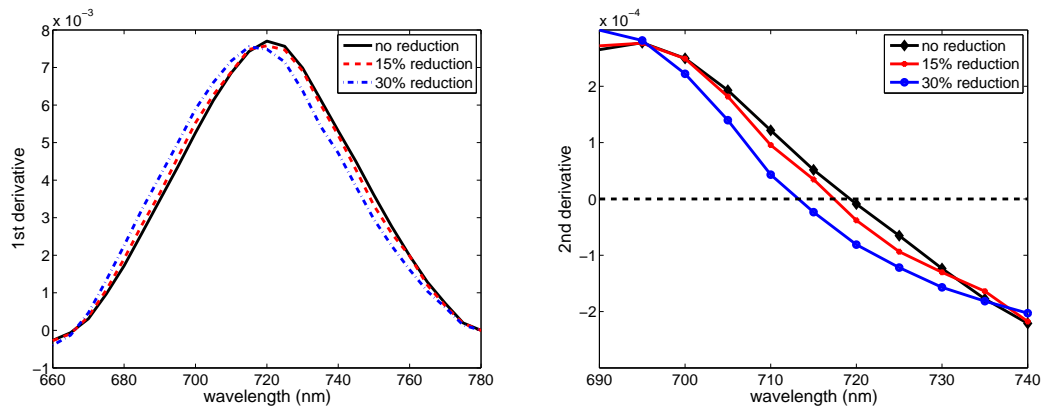

Figure 5: Simulated changes in the REP of a typical soy specimen due to nitrogen deficiency. Left: first derivative of the reflectance spectra. Right: second derivative of the reflectance spectra.

Figure 6: Simulated changes in the REP of a typical soy specimen due to moderate water reduction. Left: first derivative of the reflectance spectra. Right: second derivative of the reflectance spectra.

Specimen	Normal Conditions	Nitrogen Deficiency		Water Reduction	
		15%	30%	15%	30%
corn	720	715.75	711.75	717.25	714.25
soy	719.25	715	711	717.25	713.25

Table 1: Simulated REPs (nm) of typical corn and soy specimens subjected to nitrogen deficiency and moderate water reduction.

Specimen	Nitrogen Deficiency		Water Reduction	
	15%	30%	15%	30%
corn	4.25	4	2.75	3
soy	4.25	4	2	4

Table 2: Differences between simulated REPs (nm) of typical corn and soy specimens subjected to nitrogen deficiency and moderate water reduction.

Although the different internal arrangement of the tissues of unifacial C_4 and bifacial C_3 specimens may be responsible for their distinct REP shifts with respect to moderate water stress, one has also to consider that the specimens used in these simulations have different biophysical characteristics such as thickness and pigment content. Hence, to increase our scope of observations, we also considered virtual control corn and soy specimens with the same thickness and pigment contents. The values for these parameters were obtained by averaging the parameters provided in Figs. 1 and 2, which were used to characterize the typical corn and soy specimens used in our previous set of experiments. We note that the resulting values assigned for the characterization data describing the virtual corn and soy specimens are within the actual range of values measured for real corn and soy specimens.[14, 20, 21]

The results of our second set of simulations involving the virtual corn and soy specimens subjected to two different levels (15% and 30%) of nitrogen deficiency and water reduction are presented in Figs. 7 to 10 and Table 3. The same monotonic shift toward shorter wavelengths can be observed in these results. In addition, the nitrogen deficiency resulted in a similar pattern of REP shift for both specimens, albeit not quite as linear as the corresponding pattern observed in the first set of simulations. More importantly, the water reduction resulted in a similar REP shift pattern observed in the first set of simulations, namely an approximately linear decrease for the corn specimen, and an approximately quadratic decrease for the soy specimen as indicated by the REP differences presented in Table 4. These results suggest that indeed the differences in the internal arrangement of the tissues of unifacial C_4 and bifacial C_3 leaves may be responsible for their distinct REP shift patterns in response to moderate water stress. As pointed out by Govender *et al.*,[7] the influence of the internal leaf structure on plants's spectral responses to changes in water content can make the detection of low or moderate levels of plant water stress difficult. Hence, the structural differences between unifacial C_4 and bifacial C_3 plants should be carefully taken into account in the early assessment of the water-stress and in the discrimination between this condition and nutrient (nitrogen) deficiency.
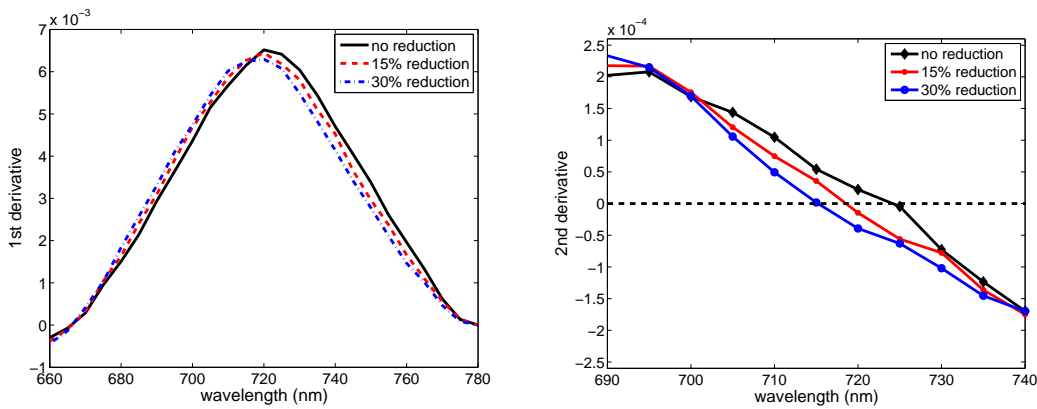

Figure 7: Simulated changes in the REP of a virtual corn specimen due to nitrogen deficiency. Left: first derivative of the reflectance spectra. Right: second derivative of the reflectance spectra.
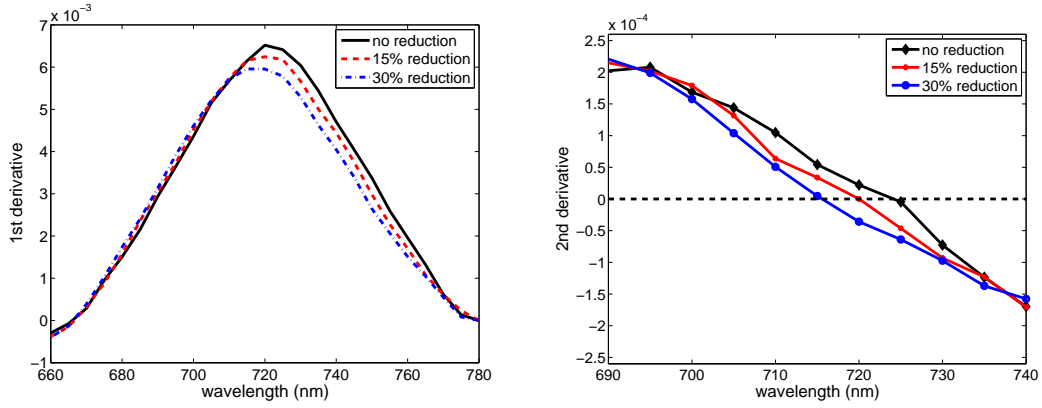
Figure 8: Simulated changes in the REP of a virtual corn specimen due to moderate water reduction. Left: first derivative of the reflectance spectra. Right: second derivative of the reflectance spectra.
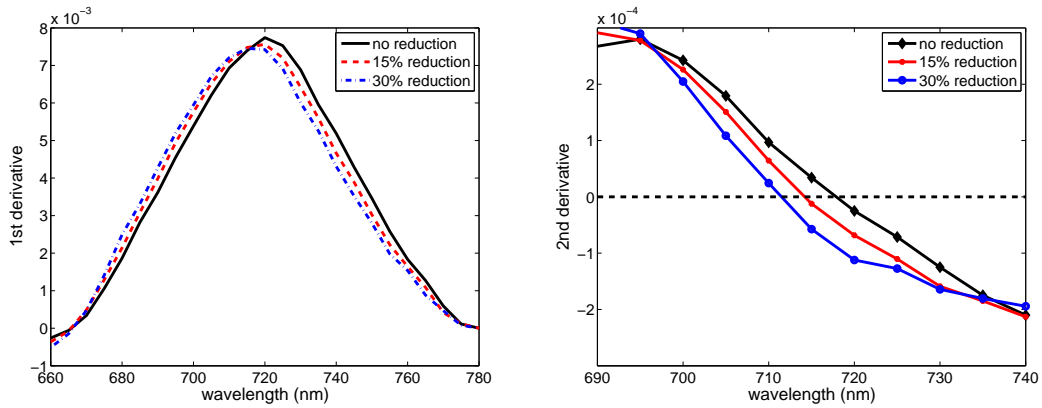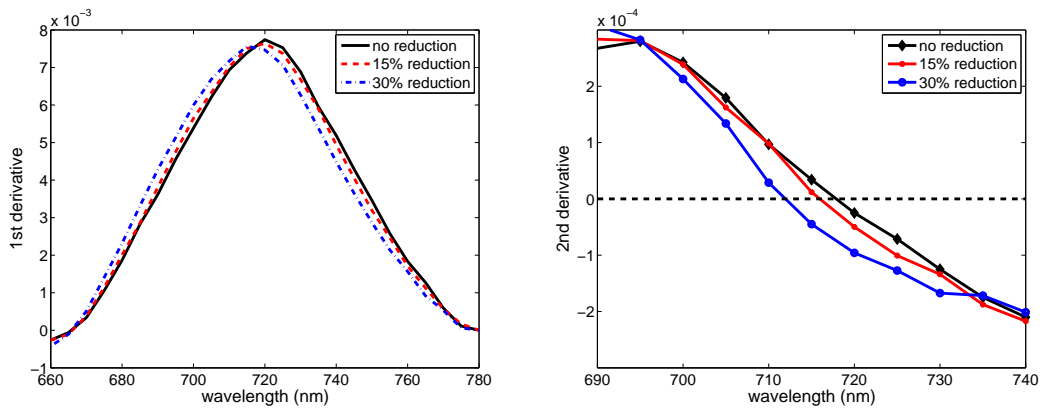

Figure 9: Simulated changes in the REP of a virtual soy specimen due to nitrogen deficiency. Left: first derivative of the reflectance spectra. Right: second derivative of the reflectance spectra.

Figure 10: Simulated changes in the REP of a virtual soy specimen due to moderate water reduction. Left: first derivative of the reflectance spectra. Right: second derivative of the reflectance spectra.

Specimen	Normal Conditions	Nitrogen Deficiency		Water Reduction	
		15%	30%	15%	30%
corn	724	718.5	715	720	715.5
soy	718	714.25	711.5	716	712

Table 3: Simulated REPs (nm) of typical corn and soy specimens subjected to nitrogen deficiency and moderate water reduction.

Specimen	Nitrogen Deficiency		Water Reduction	
	15%	30%	15%	30%
corn	5.5	3.5	4	4.5
soy	3.75	2.75	2	4

Table 4: Differences between simulated REPs (nm) of typical corn and soy specimens subjected to nitrogen deficiency and moderate water reduction.

4. CONCLUDING REMARKS

In general, investigations involving red edge shifts focus on nutrient factors affecting the pigment content of plants,[7] and data relating red edge shifts to water stress is relatively scarce in the scientific literature.[8] Even though the *in silico* experiments presented in this paper suggest distinct REP shift patterns for unifacial C_4 and bifacial C_3 plants with respect to moderate water stress, actual *in vivo* experiments are required to confirm these trends. We note, however, that similarly to other *in silico* investigations in the system biology field,[1,34] the simulation framework presented in this paper can potentially be used to accelerate the processes of hypothesis generation and validation in this area. Upon *in vivo* experimental validation, such new hypotheses can be employed in remote sensing investigations aimed at the reliable assessment of stress factors affecting C_3 and C_4 crops, notably in regions with limited access to fresh water supplies or approaching their peak productivity potential. Accordingly, we hope that the putative trends depicted in this work may contribute to the design of new effective procedures for the early detection and discrimination between nutrient and water stress, specially for important bifacial C_3 crops such as soy.

ACKNOWLEDGMENTS

REFERENCES

[1] Gutiérrez, R., "System biology for enhanced plant nitrogen nutrition," *Science* **336**, 1673–1675 (2012).

[2] Zhao, D., Reddy, K., Kakani, V., Read, J., and Carter, G., "Corn (Z*ea mays* L.) growth, leaf pigment concentration, photosynthesis and leaf hyperspectral reflectance properties as affected by nitrogen supply," *Plant and Soil* **257**, 205–217 (2003).

[3] Barnes, E., Clarke, T., Richards, S., Colaizzi, P., Haberland, J., Kostrzewski, M., Waller, P., Choi, C., Rley, E., Thompson, T., Lascano, R., Li, H., and Moran, M., "Coincident detection of crop water stress, nitrogen status and canopy density using ground-based multispectral data," in [*Fifth International Conference on Precision Agriculture*], (2000).

[4] Estep, L. and Carteri, G., "Derivative analysis of AVIRIS data for crop stress detection," *Photogrammetric Engineering & Remote Sensing* **71**(12), 1417–1421 (2005).

[5] Perry, E. and Roberts, D., "Sensitivity of narrow-band and broad-band indices for assessing nitrogen availability and water stress in an annual crop," *Agronomy Journal* **100**(4), 1211–1219 (2008).

[6] Schut, A. and Ketelaars, J., "Early detection of drought stress in grass swards with imaging spectroscopy," *NJAS* **51**(3), 319–337 (2003).

[7] Govender, M., Dye, P., Weiersbye, I., Witkowski, E., and Ahmed, F., "Review of commonly used remote sensing and ground-based technologies to measure plant water stress," *Water SA* **35**(5), 741–752 (2009).

[8] Uto, K. and Kosugi, Y., "Hyperspectral manipulation for the water stress evaluation of plants," *Contemporary Materials* **III-I**, 18–25 (2012).

[9] von Caemmerer, S., Quick, W., and Furbank, R., "The development of C_4 rice: current progress and perspectives," *Science* **336**, 1671–1672 (2012).

[10] Sage, R. and Zhu, X., "Exploiting the engine of C$_4$ photosyntheis," *Journal of Experimental Biology* **62**(9), 2989–3000 (2011).

[11] Dobrowski, S., Pushnik, J., Zarco-Tejada, P., and Ustin, S., "Simple reflectance indices track heat and water stress-induced chnages in steady-state chlorophyll fluorescence at the canopy scale," *Remote Sensing of Environment* **97**, 403–414 (2005).

[12] Railyan, V. and Korobov, R., "Red edge structure of canopy reflectance spectra of triticale," *Remote Sensing of Environment* **46**, 173–182 (1993).

[13] Baranoski, G. and Rokne, J., "A practical approach for estimating the red edge position of plant leaf reflectance," *International Journal of Remote Sensing* **26**(3), 503–521 (2005).

[14] Baranoski, G., Dimson, T., Chen, T., Kimmel, B., Yim, D., and Miranda, E., "Rapid dissemination of light transport models on the web," *IEEE Computer Graphics & Applications* **32**(3), 10–15 (2012).

[15] Baranoski, G., "Modeling the interaction of infrared radiation (750 to 2500 nm) with bifacial and unifacial plant leaves," *Remote Sensing of Environment* **100**, 335–347 (2006).

[16] Baranoski, G. and Eng, D., "An investigation on sieve and detour effects affecting the interaction of collimated and diffuse infrared radiation (750 to 2500 nm) with plant leaves," *IEEE Transactions on Geoscience and Remote Sensing* **45**, 2593–2599 (2007).

[17] NPSG, *Run ABM-B Online.* Natural Phenomena Simulation Group, University of Waterloo, Canada (2011). http://www.npsg.uwaterloo.ca/models/ABMB.php.

[18] NPSG, *Run ABM-U Online.* Natural Phenomena Simulation Group, University of Waterloo, Canada (2011). http://www.npsg.uwaterloo.ca/models/ABUB.php.

[19] NPSG, *Plant Leaf Data.* Natural Phenomena Simulation Group, University of Waterloo, Canada (2011). http://www.npsg.uwaterloo.ca/data/leaves.php.

[20] Eng, D. and Baranoski, G., "The application of photoacoustic absorption spectral data to the modeling of leaf optical properties in the visible range," *IEEE Transactions on Geoscience and Remote Sensing* **45**, 4077–4086 (2007).

[21] Hosgood, B., Jacquemoud, S., Andreoli, G., Verdebout, J., Pedrini, G., and Schmuck, G., "Leaf optical properties experiment 93," Tech. Rep. Report EUR 16095 EN, Joint Research Center, European Comission, Institute for Remote Sensing Applications (1995).

[22] Baranoski, G., Kimmel, B., Chen, T., and Yim, D., "In silico assessment of environmental factors affecting the spectral signature of C4 plants in the visible domain," *International Journal of Remote Sensing* **33**(4), 1190–1213 (2012).

[23] Loreto, F., Baker, N., and Ort, D., "Chloroplast to leaf," in [*Photosynthetic Adaptation Chloroplast to Landscape*], Smith, W., Vogelmann, T., and Critchley, C., eds., ch. 9, 231–261, Springer, NY, USA (2004). Part 6: Environmental Constraints, Ecological Studies, Vol. 178.

[24] Alberte, R. and Thornber, J., "Water stress effects on the content and organization of chlorophyll in mesophyll and bundle sheath chloroplasts of maize," *Plant Physiology* **59**, 351–353 (1977).

[25] Hendry, G., Houghton, J., and Brown, S., "The degradation of chlorophyll - a biological enigma," *New Phytologist* **107**, 255–302 (1987).

[26] Woolley, J., "Change of leaf dimensions and air volume with change in water content," *Plant Physiology* **41**, 815–816 (1973).

[27] Woolley, J., "Reflectance and transmittance of light by leaves," *Plant Physiology* **47**, 656–662 (1971).

[28] Masoni, A., Ercoli, L., and Mariotti, M., "Spectral properties of leaves deficient in iron, sulfur, magnesium and manganese," *Agronomy Journal* **88**, 937–943 (1996).

[29] Jørgensen, N., *Study on Line Imaging Spectroscopy as a Tool for Nitrogen Diagnostics in Precision Farming*, PhD thesis, Department of Agricultural Sciences, The Royal Veterinary and Agricultural University, Copenhagem, Denmark (April 2002).

[30] Lee, W., Searcy, S., and Kataoka, T., "Assessing nitrogen stress in corn varieties of varying color," in [*ASAE Annual International Meeting*], 1–24, ASAE, Toronto, Ontario, Canada (July 1999). Paper 99-3034.

[31] Buckley, T., Miller, J., and Farquhar, G., "The mathematics of linked optimization for water and nitrogen use in canopy," *Silva Fennica* **36**(3), 639–689 (2002).

[32] Carter, G. and Knapp, A., "Leaf optical properties in higher plants: linking spectral characteristics to stress and chlorophyll concentration," *American Journal of Botany* **88**(4), 677–684 (2001).

[33] Gerald, C. and Wheatley, P., [*Applied Numerical Analysis*], Addison-Wesley, Reading, Massachusetts, 6th ed. (1999).

[34] Minorsky, P., "Achieving the *in silico* plant. Systems biology and the future of plant biological research," *Plant Physiology* **132**, 404–409 (2003).